2021 IEEE International Conference on Autonomous Systems (ICAS) | 978-1-7281-7289-7/21/$31.00 ©2021 IEEE | DOI: 10.1109/ICAS49788.2021.9551195

DIFFERENCE CO-CHIRPS-BASED NON-UNIFORM PRF AUTOMOTIVE FMCW RADAR

Lifan Xu[1], *Shunqiao Sun*[1] *and Kumar Vijay Mishra*[2]

[1]Department of Electrical and Computer Engineering, The University of Alabama, Tuscaloosa, AL 35487
[2]United States CCDC Army Research Laboratory, Adelphi, MD 20783

ABSTRACT

We propose an automotive radar system that transmits at non-uniform pulse repetition frequency (PRF) to achieve high-resolution range and Doppler estimation while transmitting sparsely along slow-time following the difference co-chirps schemes, e.g., coprime and nested chirps. At the receiver, the radar admits undersampled slow-time signals for Doppler estimation. In a single coherent processing interval (CPI), the missing Doppler samples along slow-time are interpolated via a Doppler covariance matrix that is constructed using fast-time samples. Our *co*-chirp joint range-*D*oppler estimation with *D*opp*ler* de-aliasing (CoDDler) algorithm jointly estimates the range and Doppler. The Doppler spectrum obtained from the interpolated Doppler samples are utilized to de-aliase any false Doppler peaks in the sparse estimation. The proposed non-uniform PRF automotive radar provides the possibility for transmission coordination in a time division multiplexing fashion to avoid mutual interference by saving nearly 88% of time-on-target.

Index Terms— Automotive radar, difference co-chirps, FMCW, non-uniform PRF, sparse reconstruction.

1. INTRODUCTION

Automotive radar systems exploit frequency modulated continuous wave (FMCW) signals at millimeter-wave frequencies to enable high-resolution target range and velocity estimation while using a lower cost and simpler hardware than a light detection and ranging (LiDAR) system [1–4]. As more vehicles are equipped with automotive radar operating within the same 76-81 GHz frequency band, the mutual interference among automotive radars becomes severe. The mutual interference will decrease the detection performance of automotive radar. Many techniques have been proposed to mitigate the interference. The simplest way is to notch out the corrupted samples caused by the interference [3] or transmit multi-purpose waveforms [5, 6]. An alternative is to schedule the radar operation time such that mutual coherence is avoided [7, 8]. However, this strategy would result in loss of useful dwell time on targets. This is addressed through transmitting chirps sparsely along slow-time and then employ sparse reconstruction techniques to recover the targets [9–11]. Such a strategy has potential to coordinate the transmission among multiple automotive radars to avoid or greatly reduce mutual interference without loss of performance.

In this context, radar waveforms that transmit at non-uniform pulse repetition frequency (PRF) have been developed in [10, 12–14]. In [12], a weight interpolation technique was considered to handle the high sidelobes in the Doppler spectrum caused by non-uniform pulsing. In [13], after interpolation to suppress these sidelobes, the non-uniform pulses are processed via non-uniform fast Fourier transform (NUFFT). A direct interpolation of Fourier coefficients is avoided in [10] by employing the compressed sensing (CS) technique to recover the Doppler information. Optimal pulse transmission structure and sampling rules were considered in [14] to control the sidelobe level of Doppler spectrum.

In this context, there is a rich heritage of research on non-uniform sampling in the spatial domain, e.g., using sparse arrays [15, 16]. For example, difference coarray concept has been exploited for direction of arrival (DOA) estimation in passive sensing. Some well-known difference coarrays include the minimum redundancy array (MRA) [17], nested array [18], coprime array [19–21], and super nested array [22, 23]. When a sufficient number of snapshots are available, the difference coarray concept is utilized to construct a coarray with significantly increased virtual sensors from a sparse physical array [24]. Difference coarray concept has been utilized for spectrum estimation of a wide sense stationary (WSS) process with significantly reduced sampling rate [25]. In the automotive sensing scenario, however, the environment is highly dynamic [26]. The positions of radar-mounted vehicle and objects often change rapidly [3].

In this paper, we exploit the concept of difference coarray for automotive radar waveform design. We propose *difference co-chirps* for an FMCW radar, where a coherent processing interval (CPI) comprises a sparse chirp sequence following the co-chirp concept instead of a a consecutive chirp sequence along slow-time with a high PRF. At the receiver, we sparsely sample the radar signals along slow-time. In order to jointly recover the range and Doppler, we adopt a two-dimensional CS (2D-CS) algorithm followed by a Doppler de-aliasing step. The missing samples along the slow-time are filled via the sampling covariance matrix that is constructed using the fast-time samples. The filled slow-time samples are utilized to de-aliasing any false Doppler peaks in the CS estimation. Our proposal does not rely on multiple snapshots from multiple CPIs. Furthermore, it allows the transmission coordination among multiple automotive radars to avoid potential mutual interference.

The rest of the paper is organized as follows. In the next section, we introduce the conventional uniform PRF and our proposed co-chirp FMCW radars. In Section 3, we describe our *co*-chirp joint range-*D*oppler estimation with *D*opp*ler* de-aliasing (CoDDler) procedure for the co-chirp radar. We validate our models and methods through numerical experiments in Section 4. We conclude in Section 5. Throughout this paper, upper-case and lower-case bold characters denote matrices and vectors respectively. Matrix vectorization operation is denoted by $\mathrm{vec}(\cdot)$. The conjugate transpose is $(\cdot)^H$. The complex values set is $\mathbb{C}$. The ceiling operation is denoted by $\lceil\cdot\rceil$.

2. SYSTEM MODEL

We briefly describe the conventional FMCW radar and follow with the difference co-chirp system.

2.1. State-of-the-art FMCW radar

Consider a monostatic FMCW radar that transmits a linear frequency ramp. The transmit signal for one ramp at m-th chirp with bandwidth B and the duration time T is

$$s(m,t) = \text{rect}\left(\frac{t-mT_p}{T}\right) e^{\text{j}2\pi\left[f_c+\frac{B}{T}(t-mT_p)\right](t-mT_p)}, \quad (1)$$

where T_p denotes the pulse repetition interval (PRI) and

$$\text{rect}\left(\frac{t-\tau}{T}\right) = \begin{cases} 1, & \tau \le t \le \tau+T \\ 0, & \text{otherwise.} \end{cases} \quad (2)$$

The phase of the transmit signal $s(m,t)$ is

$$\begin{aligned}\varphi_T\left(t-mT_p\right) =& 2\pi \int_{mT_p}^{mT_p+t} \left[f_c + \frac{B}{T}(t-mT_p)\right] dt \\ =& 2\pi\left(f_c t + \frac{1}{2}\cdot\frac{B}{T}t^2\right) - \varphi_{T_0}, \end{aligned} \quad (3)$$

where φ_{T_0} is the initial phase. We consider K_u noncoherent signals and P_c coherent signals in far field. The delayed version of transmit signal is the noiseless received signal

$$\begin{aligned} y(t) = &\sum_{k_u=1}^{K_u} \alpha_{k_u} e^{\text{j}2\pi\left[f_c(t-\tau_{k_u})+\frac{B}{2T}(t-\tau_{k_u})^2\right]} \\ &+ \sum_{p_c=1}^{P_c} \alpha_{p_c} e^{\text{j}2\pi\left[f_c(t-\tau_{p_c})+\frac{B}{2T}(t-\tau_{p_c})^2\right]}, \end{aligned} \quad (4)$$

where α_{k_u} (τ_{k_u}) and α_{p_c} (τ_{p_c}) denotes the reflection coefficients (time delays) of noncoherent and coherent signals, respectively.

The above received signal is first de-chirped with the transmit signal. The de-chirped signal is called beat signal, whose phase is

$$\Delta\varphi(t) = \varphi_T(t) - \varphi_T(t-\tau_k) = 2\pi\left(f_c\tau_k + \frac{B}{T}t\tau_k - \frac{B}{2T}\tau_k^2\right), \quad (5)$$

where τ_k denotes the delay between the transmitted and received signal of k-th target. The square term of time τ_k in the equation (5) is negligible in short range automotive radars since it typically holds that $\tau_k/T \ll 1$. Here, in the de-chirped signal, t starts from zero for each chirp.

Assume the k-th target has range of r_k with constant velocity v_k. Then, the round-trip transmission delay for the k-th target is $\tau_k = 2(r_k + v_k t)/c$, where c is the speed of light. The phase of the de-chirp signal is

$$\Delta\varphi(t) = 2\pi\left[\frac{2f_c r_k}{c} + \left(\frac{2f_c v_k}{c} + \frac{2Br_k}{cT}\right)t + \frac{2Bv_k}{cT}t^2\right], \quad (6)$$

where $\frac{2Bv_k}{Tc}t^2$ is negligible in typical automotive radars and $\frac{2f_c r_k}{c}$ is a constant phase that can be absorbed into the reflection coefficients α_{k_u} or α_{p_c}. The beat frequency of the k-th target is $f_b^k = f_R^k + f_D^k$, where $f_R^k = \frac{2Br_k}{Tc}$ and $f_D^k = \frac{2f_c v_k}{c}$ are, respectively, range and Doppler frequencies of the k-th target.

In automotive radars with maximum detection range of hundreds of meters, it holds that $f_b \ll B$. As a result, the beat signals can be sampled using a much cheaper low-rate analog-to-digital converter (ADC). Assume T_A denotes the sampling interval in fast-time and $1/T_A > 2f_b^{\max}$, where $f_b^{\max}$ denotes the maximum beat frequency. The i-th sample in the m-th chirp is

$$\begin{aligned} y(m,i) = &\sum_{k_u=1}^{K_u} \alpha_{k_u} e^{\text{j}2\pi\left(f_b^{k_u} iT_A + f_D^{k_u} mT_p\right)} + \\ &\sum_{p_c=1}^{P_c} \alpha_{p_c} e^{\text{j}2\pi\left(f_b^{p_c} iT_A + f_D^{p_c} mT_p\right)}. \end{aligned} \quad (7)$$

Assume a CPI consists of M chirps and number of samples in each chirp is I. The sampled automotive radar data cube is denoted by $\mathbf{Y} \in \mathbb{C}^{I\times M}$ whose entries are $y(m,i)$.

For a typical automotive radar, it holds that $f_D \ll f_R$. Thus, the Doppler frequency f_D is negligible in a single chirp and range is estimated by applying fast Fourier transform (FFT) along fast-time samples in the above-mentioned data cube. For each range bin, the range frequency f_R is constant across the slow-time. Thus, the Doppler is estimated by applying FFT along the slow-time in data cube $\mathbf{Y}$ [3]. To avoid ambiguity in Doppler spectrum estimation in uniform PRF radar, it is required that $f_{\text{PRF}} \ge 2f_D^{\max}$, where $f_{\text{PRF}} = 1/T_p$ is the PRF of chirps and $f_D^{\max}$ denotes the maximum Doppler frequency.

In this paper, instead of transmitting a uniform chirp sequence with a high PRF, we propose an automotive radar system that transmits a non-uniform chirp sequence in each CPI following the co-chirp concept, such as coprime chirps and nested chirps. The challenge lies in that the non-uniform PRF violates the Nyquist sampling rate for Doppler estimation thereby leading to high sidelobes in the Doppler spectrum. Our goal is to develop high-resolution algorithm to jointly estimate range and Doppler under the difference co-chirps concept while avoiding Doppler ambiguity.

2.2. Difference co-chirp based FMCW radar

Consider a chirp set $\mathbb{S}_1 = \{m_1, m_2, ..., m_M\}$, which has M chirp entries. Let m_i denote the i-th chirp. The set of difference chirp indices is

$$\mathbb{S}_{\text{diff}} = \{m_i - m_j\}, \qquad \forall i,j \in \mathbb{S}_1 \quad (8)$$

In this difference co-chirps set, the entries occur only once.

2.2.1. FMCW radar with coprime chirps scheme

Consider an FMCW radar that transmits along the slow-time according to coprime chirps relationship. Two coprime numbers N_1 and N_2 are used to define a chirps slow-time slot set as

$$\begin{aligned} &\mathbb{S}_{\text{coprime}} = \\ &\{N_1 n_2, 0 \leqslant n_2 \leqslant N_2 - 1\} \cup \{N_2 n_1, 0 \leqslant n_1 \leqslant N_1 - 1\}. \end{aligned} \quad (9)$$

A FMCW chirp will be transmitted at the slow-time indices specified in the above set. The difference co-chirps set is

$$\mathbb{S}_{\text{diff}} = \{s_1 - s_2 | s_1, s_2 \in \mathbb{S}_{\text{coprime}}\}. \quad (10)$$

However, the difference co-chirps set does not include consecutive chirps from time slots $-N_2(N_1-1)$ to $N_1(N_2-1)$, and certain chirp indices are missing (see Fig. 1(b)).

2.2.2. FMCW radar with nested chirps scheme

We now examine the FMCW radar that sends pulses along the slow-time following the nested chirps relationship. Two-level chirp indices are used in nested chirps scheme. Specifically, the first and second levels consist of N_1 and N_2 chirps with corresponding PRIs as T_p and $(N_1+1)T_p$, respectively. Under the nested chirps scheme,

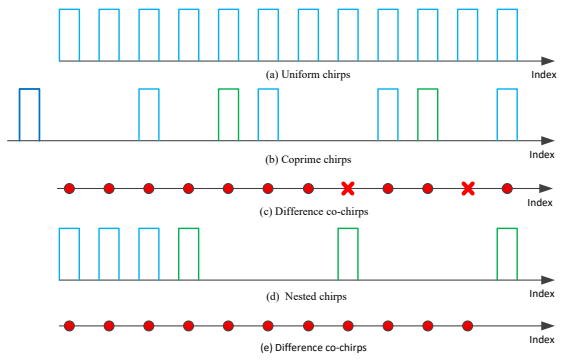

Fig. 1. Different non-uniform chirps schemes and their difference co-chirps.The missing chirp indices are denoted by ×, while the filled difference chirp indices are denoted by •. (a) The uniform PRF chirps. (b) The coprime chirps scheme for $N_1 = 3, N_2 = 5$. (d) The nested chirps scheme for $N_1 = 3, N_2 = 3$.

FMCW radar transmit chirps at slow-time indices as per the set

$$\mathbb{S}_{\text{nested}} = \{1, 2, \cdots, N_1, (N_1+1), 2(N_1+1), \cdots, N_2(N_1+1)\}. \quad (11)$$

The set $\mathbb{S}_{\text{diff}} = \{n_1 - n_2 | n_1, n_2 \in \mathbb{S}_{\text{nested}}\}$ is called the difference of nested-chirps. The set containing unique chirp (UC) listed in $\mathbb{S}_{\text{diff}}$ is denoted as $\mathbb{S}_{\text{diff}}^{\text{UC}}$ (see Fig. 1(c)), where total transmitted chirps are $N = N_1 + N_2$. Under the nested scheme, the first N_1 transmitted chirps have PRI of T_p while the second N_2 chirps have PRI of $(N_1+1)T_p$. The sampled beat signal at the m-th chirps can be expressed in (7) for $m \in \mathbb{S}_{\text{nested}}$.

The Doppler velocity resolution is determined by the length of a CPI. To achieve the same Doppler resolution as uniform PRF scheme, FMCW radar under difference co-chirps schemes need to transmit over the whole CPI sparsely along the slow-time following the corresponding coprime or nested co-chirp rules. In Fig. 1, total 12 chirps need to be transmitted under the uniform PRF scheme in one CPI. On the other hand, for the same observation window time, only 8 and 6 chirps need to be transmitted under the coprime and nested chirp strategies, respectively.

3. JOINT RANGE AND DOPPLER ESTIMATION

We develop super-resolution algorithm CoDDler to jointly estimate the range and Doppler when FMCW chirps are transmitted sparsely along slow-time following the difference nested-chirps rule. Note that high sidelobes of the Doppler spectrum arising from the sparse sampling pose a challenge here. Our 2D-CS algorithm jointly estimates the range and Doppler using the sparse samples along slow-time. To remove the Doppler ambiguity, we devise a difference co-chirps interpolation based Doppler de-aliasing strategy.

Assume R_u and $v_{\max}$ denote the maximum detection range and velocity, respectively. To construct an appropriate CS dictionary [27, 28], the range and velocity are discretized into a fine grid with $M_r \times M_v$ points. The corresponding range and velocity grid sizes are $\frac{R_u}{M_r}$ and $\frac{2v_{\max}}{M_v}$, respectively. The ξ-th range and η-th discretized velocity are denoted as R_ξ and v_η. The corresponding beat frequency is $f_b^{\xi\eta} = f_R^\xi + f_D^\eta$. The corresponding constructed noise-free data matrix is denoted by $\mathbf{Z}_{\xi\eta} \in \mathbb{C}^{I \times N}$ whose elements are

$$z(n,i) = e^{\text{j}2\pi\left(f_b^{\xi\eta} i T_A + f_D^\eta n T_p\right)}, n \in \mathbb{S}_{\text{nested}}. \quad (12)$$

The dictionary of the 2D-CS is

$$\mathbf{A} = [\text{vec}(\mathbf{Z}_{11}), \cdots, \text{vec}(\mathbf{Z}_{1M_v}), \text{vec}(\mathbf{Z}_{21}), \cdots, \text{vec}(\mathbf{Z}_{M_r M_v})]. \quad (13)$$

In practice, the measurement is corrupted with noise, i.e., $\text{vec}(\mathbf{Y}) = \mathbf{A}\mathbf{x} + \mathbf{n}$, where $\mathbf{n}$ is the noise vector. Here, $\mathbf{x} \in \mathbb{C}^{M_v M_r \times 1}$ is a sparse vector, where $x_j = \alpha_h$ with $h = K_u$ or $h = P_c$ if the h-th target has range of $\frac{R_u}{M_r}\left\lceil \frac{j}{M_v} \right\rceil$ and velocity of $-v_{\max} + \frac{2v_{\max}}{M_v} \mod (j, M_r)$; otherwise, $x_j = 0$.

To range and Doppler, we solve the optimization problem

$$\text{minimize } \|\mathbf{x}\|_1 \quad \text{subject to } \|\text{vec}(\mathbf{Y}) - \mathbf{A}\mathbf{x}\|_2 \le \delta, \quad (14)$$

where δ is the noise bound. Some popular solvers such as Dantzig selector [29] or orthogonal matching pursuit (OMP) [30] are used to solve (14) to obtain the signal vector $\mathbf{x}$. Successful recovery of the sparse vector $\mathbf{x}$ requires that the dictionary matrix $\mathbf{A}$ has low value of its mutual coherence defined as

$$\mu(\mathbf{A}) = \max_{l \ne j} \frac{\mathbf{A}_l^{\text{H}} \mathbf{A}_j}{\|\mathbf{A}_l\|_2 \|\mathbf{A}_j\|_2}, \quad (15)$$

where $\mathbf{A}_j$ denotes the j-th column of matrix $\mathbf{A}$.

It follows that the sparse sampling along slow-time with difference co-chirps schemes leads to high sidelobes of Doppler spectrum resulting in high mutual coherence. Consequently, false Doppler detections are likely in the CS output. By utilizing the sparse samples from difference co-chirps, we interpolate the missing samples along slow-time for non-ambiguity Doppler estimation, which are then used for Doppler de-aliasing in the CS estimation output.

In each CPI, the missing samples along slow-time for Doppler estimation are interpolated via construction of a second-order covariance matrix, which requires a large number of snapshots. As mentioned earlier, the Doppler shift in a typical automotive radar is negligible during fast-time sampling of a single chirp and is viewed as a constant [3]. Therefore, we treat the fast-time samples as "snapshot" for Doppler covariance matrix construction. Following the equation (7), the i-th snapshot of slow-time samples or the i-th row of sparse radar data cube is

$$\mathbf{y}_{\text{nested}}^i = \mathbf{B}\mathbf{\Sigma}\mathbf{s}^i + \mathbf{n}^i, \quad (16)$$

where $\mathbf{B} = \left[\mathbf{b}(f_D^1), \mathbf{b}(f_D^2), \cdots, \mathbf{b}(f_D^K)\right] \in \mathbb{C}^{N \times K}$ is the Doppler manifold with $\mathbf{b}(f_D^k) = \left[e^{\text{j}2\pi f_D^k T_p}, \cdots, e^{\text{j}2\pi f_D^k N T_p}\right]^T$ and $\mathbf{s}^i = \left[e^{\text{j}2\pi f_b^k i T_A}, \cdots, e^{\text{j}2\pi f_b^k i T_A}\right]^T$. Here, $\mathbf{n}^i$ denotes the noise vector in the i-th snapshot of slow-time samples and $\mathbf{\Sigma} = \text{diag}([\alpha_1, \cdots, \alpha_K])$.

The missing Doppler samples along slow-time are interpolated via the Doppler autocorrelation $\mathbf{y}_{\text{nested}}^i \left(\mathbf{y}_{\text{nested}}^i\right)^H$, whose entries include $e^{\text{j}2\pi f_D^k (n_2 - n_1) T_p}$ for $n_1, n_2 \in \mathbb{S}_{\text{nested}}$, i.e., $e^{\text{j}2\pi f_D^k n T_p}$ for $n \in \mathbb{S}_{\text{diff}}$. From the nested-chirps properties, the indices in $\mathbb{S}_{\text{diff}}$ are consecutive. The sampling Doppler covariance matrix is

$$\mathbf{R}_{\text{nested}} = \frac{1}{I} \sum_{i=1}^{I} \mathbf{y}_{\text{nested}}^i \left(\mathbf{y}_{\text{nested}}^i\right)^H. \quad (17)$$

Let $\mathbf{d}_{\text{diff}}^{\text{UC}} = \text{unique}(\mathbf{R}_{\text{nested}})$ denote the averaged unique consecutive Doppler samples obtained from the sampling covariance matrix with indices defined in $\mathbb{S}_{\text{diff}}^{\text{UC}}$. Then, the Doppler spectrum is obtained by applying FFT on the interpolated Doppler samples along slow-time. The Doppler spectrum is accurate and robust, which indicates the targets' radar cross section (RCS). Thus, the Doppler spectrum is utilized to filter out false velocity peaks in the CS estimation. Algorithm 1 summarizes these steps.

Algorithm 1 *Co*-chirp joint range-*D*oppler estimation with *Dopp*l*er* de-aliasing (CoDDler)

Input: N_1, N_2, M_v, M_r and the received sparse data cube $\mathbf{Y}$.
Output: de-aliasing CS range-Doppler spectrum.
Doppler spectrum with interpolated Doppler samples:

1: $\mathbf{R}_{\text{nested}} = \frac{1}{I}\sum_{i=1}^{I} \mathbf{y}^i_{\text{nested}} \left(\mathbf{y}^i_{\text{nested}}\right)^H$.
2: $\mathbf{d}^{\text{UC}}_{\text{diff}} = \text{unique}\left(\mathbf{R}_{\text{nested}}\right)$.
3: $\mathcal{D} = \text{FFT}\left\{\mathbf{d}^{\text{UC}}_{\text{diff}}\right\}$.
Range-Doppler estimation with 2D-CS and Doppler de-aliasing:
4: Discretize the range and velocity into a fine grid and construct dictionary matrix $\mathbf{A}$ according to (13).
5: Solve ℓ_1 norm optimization problem (14) by OMP.
6: Apply the Doppler spectrum $\mathcal{D}$ to filter out fake velocity peaks in CS estimation.

4. NUMERICAL RESULTS

We consider a two-level nested chirps FMCW radar with carrier frequency of f_c =77 GHz, and bandwidth of B = 150 MHz. The maximum unambiguous detection range is R_u = 200 m and the maximum unambiguous velocity is $v_{\max}$ = 63.89 m/s. The sampling frequency of beat signal is $f_s = 27.3$ MHz. The PRI is $T_p = 15.2\mu$s for uniform PRF automotive radar. In a CPI, the difference co-chirps based automotive radar first transmits N_1 = 17 chirps with PRI of T_p and then N_2 = 17 chirps with PRI of $(N_1 + 1)\,T_p$. Then, there are total 305 chirps in the interpolated Doppler samples. The signal-to-noise ratio (SNR) of the beat signal is set to 10 dB. Two targets at $r_1 = 110$ m, $v_1 = 15$ m/s and $r_2 = 50$ m, $v_2 = 35$ m/s with the same RCS are considered.

The range-Doppler spectrum obtained by applying the 2D-FFT on the sparse data with nested-chirps are shown in Fig.2(a). Note that there are many high sidelobes along Doppler axis because the sparse sampling along slow-time violates the Nyquist sampling criterion. The range-Doppler estimation on the sparse data with nested-chirps using 2D-CS is plotted in Fig. 2(b). The high coherence of dictionary $\mathbf{A}$ leads to false peaks in the velocity estimation, which cannot be eliminated without prior knowledge of targets.

Fig. 2(c) plots the Doppler spectrum obtained from the interpolated Doppler samples along slow-time, which clearly show two peaks at the ground-truth locations. The threshold obtained from the Doppler spectrum is used to filter out artifacts in the 2D-CS estimation. The 2D-CS estimation after de-aliasing using Doppler spectrum is shown in Fig. 2(d), where the false peaks are mitigated.

The range-Doppler spectrum obtained by applying the 2D-FFT on the sparse data with co-prime chirps are shown in Fig. 3(a), while the range-Doppler estimation with 2D-CS on the sparse samples are plotted in Fig. 3(b). Since the interpolated Doppler samples along slow-time are not consecutive under the difference co-prime chirps scheme, there are high sidelobes in the Doppler spectrum of the interpolated Doppler samples (Fig. 3(c)), which cannot be used for Doppler de-aliasing in the 2D-CS estimation.

In both examples, a uniform PRF radar would transmit 306 chirps in a CPI. On the contrary, the difference co-chirps schemes with nested chirps and coprime chirps schemes only need 34 and 37 chirps to achieve the same Doppler resolution, respectively, with 89% and 88% savings in the dwell time, respectively.

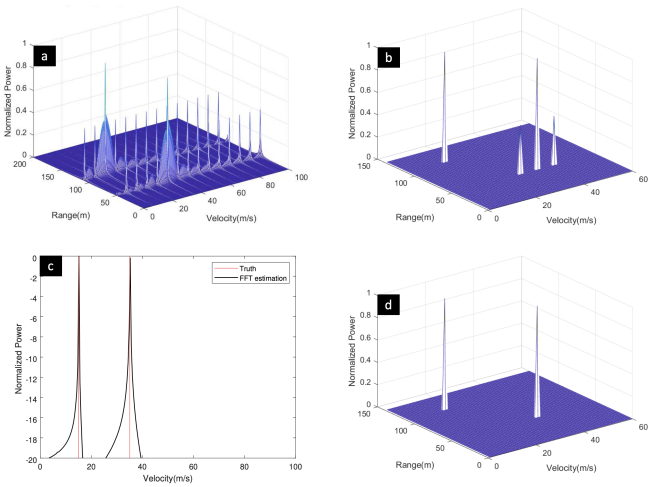

Fig. 2. Range-Doppler spectrum under the difference nested-chirps scheme. (a) 2D-FFT on the sparse samples. (b) 2D-CS on the sparse samples. (c) Doppler spectrum of the interpolated slow-time samples. (d) 2D-CS on the sparse samples after Doppler de-aliasing.

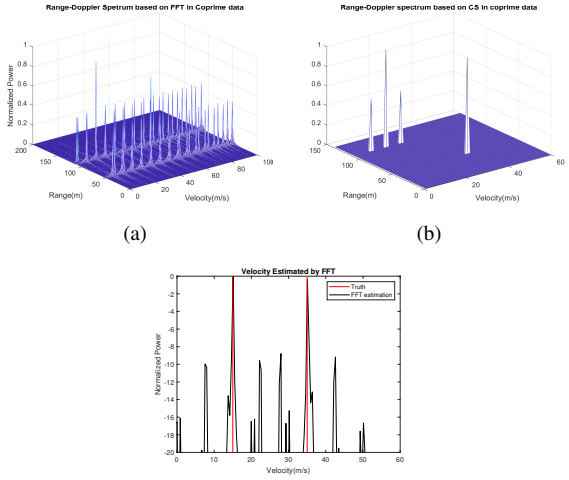

Fig. 3. Range-Doppler spectrum under the difference co-prime chirps scheme. (a) 2D-FFT on the sparse samples. (b) 2D-CS on the sparse samples. (c) Doppler spectrum of the interpolated slow-time samples.

5. SUMMARY

We proposed difference co-chirps based non-uniform PRF automotive FMCW radar that exploits the difference coarray concepts. In this approach, the automotive radar transmits sparsely in a CPI with the equivalent co-chirp determining the chirp sequence. In particular, we investigated co-prime and nested chirp sequences. Our proposed CoDDleR jointly estimates the range and Doppler from the radar signals sparsely sampled along slow-time. Numerical results demonstrated the feasibility of the proposed method in achieving high-resolution range-Doppler estimation while mitigating false Doppler peaks. The saving in the dwell time with co-chirp radar is more than 88% when compared to the uniform PRF radar.

6. REFERENCES

[1] S. Patole, M. Torlak, D. Wang, and M. Ali, "Automotive radars: A review of signal processing techniques," *IEEE Signal Processing Magazine*, vol. 34, no. 2, pp. 22–35, 2017.

[2] F. Engels, P. Heidenreich, A. M. Zoubir, F. Jondral, and M. Wintermantel, "Advances in automotive radar: A framework on computationally efficient high-resolution frequency estimation," *IEEE Signal Processing Magazine*, vol. 34, no. 2, pp. 36–46, 2017.

[3] S. Sun, A. P. Petropulu, and H. V. Poor, "MIMO radar for advanced driver-assistance systems and autonomous driving: Advantages and challenges," *IEEE Signal Processing Magazine*, vol. 37, no. 4, pp. 98–117, 2020.

[4] K. V. Mishra, M. R. Bhavani Shankar, V. Koivunen, B. Ottersten, and S. A. Vorobyov, "Toward millimeter wave joint radar-communications: A signal processing perspective," *IEEE Signal Processing Magazine*, vol. 36, no. 5, pp. 100–114, 2019.

[5] S. H. Dokhanchi, B. S. Mysore, K. V. Mishra, and B. Ottersten, "A mmWave automotive joint radar-communications system," *IEEE Transactions on Aerospace and Electronic Systems*, vol. 55, no. 3, pp. 1241–1260, 2019.

[6] G. Duggal, S. Vishwakarma, K. V. Mishra, and S. S. Ram, "Doppler-resilient 802.11ad-based ultrashort range automotive joint radar-communications system," *IEEE Transactions on Aerospace and Electronic Systems*, vol. 56, no. 5, pp. 4035–4048, 2020.

[7] S. Alland, W. Stark, M. Ali, and A. Hedge, "Interference in automotive radar systems: Characteristics, mitigation techniques, and future research," *IEEE Signal Processing Magazine*, vol. 36, no. 5, pp. 45–59, 2019.

[8] Z. Slavik and K. V. Mishra, "Cognitive interference mitigation in automotive radars," in *IEEE Radar Conference*, 2019, pp. 1–6.

[9] S. Na, K. V. Mishra, Y. Liu, Y. C. Eldar, and X. Wang, "TenD-SuR: Tensor-based 4D sub-Nyquist radar," *IEEE Signal Processing Letters*, vol. 26, no. 2, pp. 237–241, 2018.

[10] K. V. Mishra and Y. C. Eldar, "Sub-Nyquist radar: Principles and prototypes," in *Compressed Sensing in Radar Signal Processing*, A. D. Maio, Y. C. Eldar, and A. Haimovich, Eds. Cambridge University Press, 2019, in press.

[11] K. V. Mishra, S. Mulleti, and Y. C. Eldar, "RaSSteR: Random sparse step-frequency radar," *arXiv preprint arXiv:2004.05720*, 2020.

[12] M. W. Maier, "Non-uniform PRI pulse-Doppler radar," in *Southeastern Symposium on System Theory*, Tuscaloosa, AL, Mar. 7-9, 1993, pp. 164–168.

[13] J. Li and Z. Chen, "Research on random PRI PD radar target velocity estimate based on NUFFT," in *IEEE CIE International Conference on Radar*, 2011, pp. 1801–1803.

[14] W. P. Plessis, "Simultaneous unambiguous range and Doppler through non-uniform sampling," in *Proc. IEEE Radar Conf.*, Florence, Italy, Sept. 21-25, 2020.

[15] S. Sedighi, B. Shankar, K. V. Mishra, and B. Ottersten, "Optimum design for sparse FDA-MIMO automotive radar," in *Asilomar Conference on Signals, Systems, and Computers*, 2019, pp. 913–918.

[16] K. V. Mishra, I. Kahane, A. Kaufmann, and Y. C. Eldar, "High spatial resolution radar using thinned arrays," in *IEEE Radar Conference*, 2017, pp. 1119–1124.

[17] C.-Y. Chen and P. P. Vaidyanathan, "Minimum redundancy MIMO radars," in *IEEE International Symposium on Circuits and Systems*, 2008, pp. 45–48.

[18] P. Pal and P. P. Vaidyanathan, "Nested arrays: A novel approach to array processing with enhanced degrees of freedom," *IEEE Transactions on Signal Processing*, vol. 58, no. 8, pp. 4167–4181, 2010.

[19] P. P. Vaidyanathan and P. Pal, "Sparse sensing with co-prime samplers and arrays," *IEEE Transactions on Signal Processing*, vol. 59, no. 2, pp. 573–586, 2011.

[20] S. Qin, Y. D. Zhang, and M. G. Amin, "Generalized coprime array configurations for direction-of-arrival estimation," *IEEE Transactions on Signal Processing*, vol. 63, no. 6, pp. 1377–1390, 2015.

[21] M. Wang and A. Nehorai, "Coarrays, MUSIC, and the Cramér-Rao bound," *IEEE Transactions on Signal Processing*, vol. 65, no. 4, pp. 933–946, 2017.

[22] C.-L. Liu and P. P. Vaidyanathan, "Super nested arrays: Linear sparse arrays with reduced mutual coupling - Part I: Fundamentals," *IEEE Transactions on Signal Processing*, vol. 64, no. 15, pp. 3997–4012, 2016.

[23] C.-L. Liu and P. Vaidyanathan, "Super nested arrays: Linear sparse arrays with reduced mutual coupling—Part II: High-order extensions," *IEEE Transactions on Signal Processing*, vol. 64, no. 16, pp. 4203–4217, 2016.

[24] H. Qiao and P. Pal, "Guaranteed localization of more sources than sensors with finite snapshots in multiple measurement vector models using difference co-arrays," *IEEE Transactions on Signal Processing*, vol. 67, no. 22, pp. 5715–5729, 2019.

[25] S. Qin, Y. D. Zhang, M. G. Amin, and A. M. Zoubir, "Generalized coprime sampling of Toeplitz matrices for spectrum estimation," *IEEE Transactions on Signal Processing*, vol. 65, no. 1, pp. 81–94, 2017.

[26] I. Bilik, O. Longman, S. Villeval, and J. Tabrikian, "The rise of radar for autonomous vehicles: Signal processing solutions and future research directions," *IEEE Signal Processing Magazine*, vol. 36, no. 5, pp. 20–31, 2019.

[27] A. Gupta, U. Madhow, and A. Arbabian, "Super-resolution in position and velocity estimation for short-range MM-wave radar," in *Asilomar Conference on Signals, Systems and Computers*, 2016, pp. 1144–1148.

[28] M. M. Hyder and K. Mahata, "Range-Doppler imaging via sparse representation," in *IEEE Radar Conference*, 2011, pp. 486–491.

[29] E. J. Candès and T. Tao, "The Dantzig selector: Statistical estimation when p is much larger than n," *The Annals of Statistics*, vol. 35, no. 6, pp. 2313–2351, 2007.

[30] T. T. Cai and L. Wang, "Orthogonal matching pursuit for sparse signal recovery with noise," *IEEE Transactions on Information Theory*, vol. 57, no. 7, pp. 4680–4688, 2011.